Wind Tunnel Test of an Unmanned Aerial Vehicle (UAV)

Chung Jindeog*
Korea Aerospace Research Institute, Senior Engineer,
P.O. Box 113, Yusung, Daejon, 305-600, Korea
Lee Jangyeon, Sung Bongzoo, Koo Samok
Korea Aerospace Research Institute, Principle Engineer,
P.O. Box 113, Yusung-Gu Daejon 305-600, Korea

A low speed wind tunnel test was conducted for full-scale model of an unmanned aerial vehicle (UAV) in Korea Aerospace Research Institute (KARI) Low Speed Wind Tunnel (LSWT). The purpose of the presented paper is to illustrate the general aerodynamic and performance characteristics of the UAV that was designed and fabricated in KARI. Since the testing conditions were represented minor portions of the load-range of the external balance system, the repeatability tests were performed at various model configurations to confirm the reliability of measurements. Variations of drag-polar by adding model components such as tails, landing gear and test boom are shown, and longitudinal and lateral aerodynamic characteristics after changing control surfaces such as aileron, flap, elevator and rudder are also presented. To explore aerodynamic characteristics of an UAV with model components build-up and control surface deflections, lift curve slope, pitching moment variation with lift coefficients and drag-polar are examined. The discussed results might be useful to understand the general aerodynamic characteristics and drag pattern for the given UAV configuration.

Key Words : Wind Tunnel Test, UAV, Drag Build-up, Longitudinal Stability, Control Surfaces

1. Introduction

Wind tunnel test of an UAV was conducted in KARI LSWT. To measure the aerodynamic and performance characteristics of an UAV, the deflection angles of control surface such as elevator, flap, aileron and rudder were changed, and the angle of attacks and yaws were varied to simulate flight conditions. Also the drag build-up by adding model components-horizontal and vertical tails, landing gear and test boom-was gauged.

The benefits offered by UAVs to the civilian and military roles are numerous in these days, and wind tunnel tests of the unconventional concepts of UAVs, especially Canard Rotor/Wing (CRW), had been performed. Bass, S. M., Thompson, T. L., Rutherford, J. W. (1993) compared drag difference between conventionally arranged horizontal and T-tail configuration, longitudinal stability in cruise mode, and control derivatives. Recently Helwani, M., Shockey, G. A., Smith, R. L., Thompson, T. L., (2001) conducted wind tunnel test of 75% scale of Dragonfly CRW and showed the aerodynamic characteristics for complete flight envelope including hovering, low speed helicopter flight and fixed-wing flight conditions.

The image system approach, commonly used as a standard way in the process of using external balance, to measure precise forces and moments exerted on the model itself did not apply in this test since the model was originally designed to perform R/C test and the customer of the wind

* Corresponding Author,
E-mail : jdchung@kari.re.kr
TEL : +82-42-860-2322; **FAX** : +82-42-860-2604
Korea Aerospace Research Institute, Senior Engineer, P.O. Box 113, Yusung, Daejon, 305-600, Korea. (Manuscript **Received** October 28, 2002; **Revised** February 6, 2003)

tunnel test desired to see basic characteristics of UAV as early as possible. The flow angularity and interference drag due to model supports and fairings are utilized from the previously measured data in which obtained when the forward swept wing model was installed as a tandem configuration.

The purpose of this paper is to show aerodynamic characteristics of an UAV, designed and fabricated in KARI. The presented data show the longitudinal, lateral and directional characteristics based upon control surface deflections. And drag-polar by adding model components is also presented.

2. Model Description and Test Conditions

A full-scale model of the UAV was used for the wind tunnel test. To measure the aerodynamic characteristics and drag-polar for various configurations, the initial test of UAV is started from wing+body [WB] configuration. The flap deflections were set 20 and 30 degrees, and the elevator deflection conditions were −10, −20, 10 and 20 degrees. The aileron setting conditions were only considered in two cases; 10/−10 and −10/10. Since the rudder of the vertical tail had an unusual configuration, only left-hand-side of vertical tail can be deflected, the effects of the rudder on UAV characteristics could be measured 0/20 and 0/−20 conditions. Table 1 lists the deflection conditions of the control surfaces.

Table 2 shows the geometric characteristics of the UAV model. The pusher-type propeller at the aft part of fuselage was installed in actual model. However, the power effect test of this model was not conduct due to the external balance signal fluctuations caused by the piston engine vibration.

Table 1 Control surface deflections

Flap	20, 30
Elevator	−20, −10, 10, 20
Aileron	−10/10, 10/−10
Rudder	0/20, 0/−20

The model supporting positions of UAV test were slightly different comparing with the conventional airplane configuration, one pitch-rod and two bayonets under the wing. Pitch-rod, which provided angle-of-attack motion to model, was positioned fore-body of model as shown in Fig. 1. A center bayonet, which is positioned in fuselage center and provided a pivoting motion of the model, was located 500 mm downstream of the pitch-rod. The inclinometer used to measure model angle-of-attack was installed inside of model spine-block, and the signal-line was routed along the slot of the pitch-rod.

The wind tunnel test section is 3×4 m (height×width) and 10 m long. The general characteristics of KARI LSWT including static and dynamic pressure uniformity, axial pressure gradient, turbulence intensity, flow angularity, and boundary layer thickness were discussed by Arnette et al (2000). The tests were run at a target velocity of 20 m/s which is in turn corresponding to Reynolds number 2.8×10^5. Static force and moment data of the model configurations were

Table 2 Model geometric characteristics

Wing Reference Area	0.688 m^7
Wing MAC	0.218 m
Wing Span	3.2 m
Horizontal Tail Area	0.08 m^2
Horizontal Tail Span	0.8 m
Fuselage Length	1.7 m

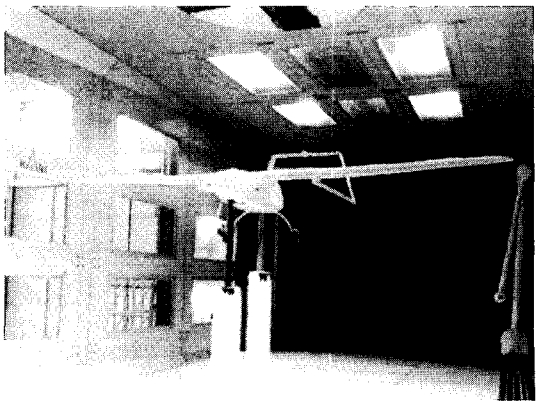

Fig. 1 Side-View of UAV Model

Table 3 Expected measurement errors

Load Components	Expected Errors
Lift Force	0.0264
Drag Force	0.0079
Side Force	0.0264
Pitching Moment	0.0546
Yawing Moment	0.0037
Rolling Moment	0.0025

(Note) The above results are obtained according to external balance resolution.

measured using a pyramidal type external 6-component strain-gauge balance. The available resolution of balance is 0.02% of full load range. Lift and drag forces, for example, can be precisely measured up to 3.92 N and 1.18 N, respectively. To eliminate thermal hysterisis effects on the balance signal, the whole balance is enclosed with thermal panel, and temperature and humidity are always kept at constant condition by an A/C unit.

With considering the current testing conditions, i.e. dynamic pressure and model geometric data, the expected errors from the external balance system are summarized in Table 3. To maintain 99.9% of confidence level with having minimal bit of A/D conversion rate, the data acquiring time was set 10 second, i.e. 50 points of data for one polar point, throughout in this test. And results of data confidence level were also checked in pre-test periods and actual data runs.

Each polar was consisted of 19 data points, and the test was conducted over an angle-of-attack range from -7 to 16 degrees. To find a precise minimal drag coefficient for the given model configuration, 0.5 degree of angle-of-attack step increases was selected from -4.5 to -3 degrees, and the rest of angle-of-attack regions was increased 1 or 2 degree step. Since the UAV model test was performed at a relatively low dynamic pressure condition, the fan RPM change discussed by Chung et al (2002) was not necessary. The average dynamic pressure of the model test was 226.8 Pa, and the standard deviation of dynamic pressure was 2.1 Pa.

3. Results and Discussion

The aerodynamic characteristics of an UAV including control surfaces deflections were measured by using external balance system. As mentioned previously, the interference drag and flow angularity of the bi-pod model arrangement were obtained from the previously performed forward swept wing model test. In that test, the model supports such as pitch-rod and center bayonet were exactly same size, the dynamic pressure of the test was however set 7 times higher than the current test. To correctly subtract the interference drag, the extra test increasing the testing speed up to 50 m/s, which is corresponding to the forward swept model test was executed. With having the correction quantities and flow angularity that is 0.14 degrees, the blockage, wall interference, weight tare and interference drag were applied for the measured data.

Before starting data comparisons, the confidence of the measurement will be discussed with repeatability test. The aerodynamic characteristics by adding model component such as vertical and horizontal tails, landing gear and test boom are discussed, and the variation of aerodynamic coefficients due to the control surface deflections are also presented.

3.1 Repeatability test

Since the testing dynamic pressure and model geometric characteristics were restricted the accuracy of the external balance, discussed in Table 3, repeatability tests of the various model configurations was the only means to validate the quality of measured results. And the repeatability tests for various configurations were performed several times irrespective of test condition. Also through out the UAV model test, if the measured quantities and data patterns are not coincided with expected trend, the model position is returned and took data again.

The model configuration used for repeatability test was consisted of the wing, vertical and horizontal tails, and fuselage with test boom attached at model nose section shown in Fig. 2, and the

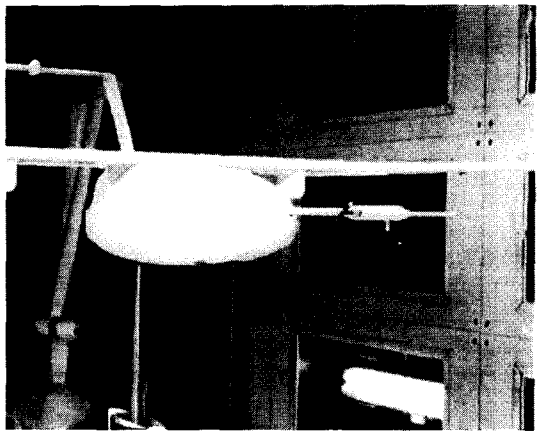

Fig. 2 Test boom Installation

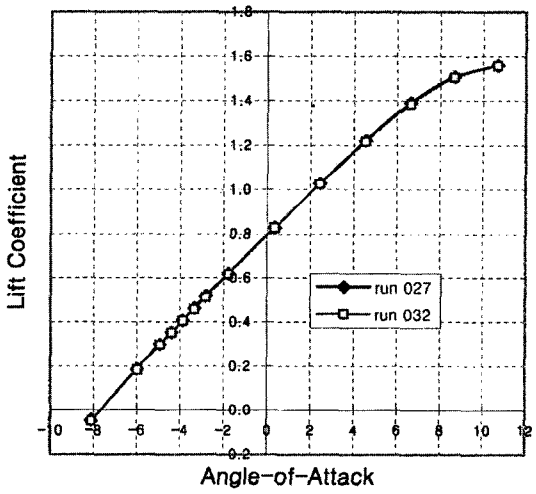

Fig. 3 Lift repeatability

control surfaces of the model were fixed at zero degree of deflection angle. Figures 3 through 5 present results of test with two days of time interval, and those results are only used to show the repeatability of the measured data, that is data corrections were not applied.

The Fig. 3 shows result of repeatability test for the lift coefficient and angle-of-attack. At the single glance, two runs seem to have identical lift slope and values. To explore the accuracy of the repeatability test, the 3rd order of spine curve fitting was applied in a limited angle-of-attack range, from −6 degrees to 7 degrees. The average difference is 17 counts, which is 0.26 N. The wing tip of the model was bent upward and showed a

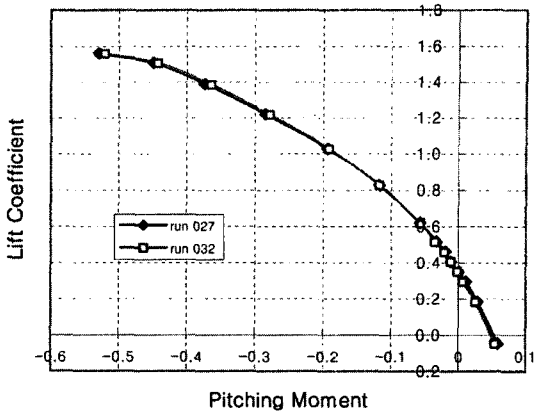

Fig. 4 P.M. and lift repeatability

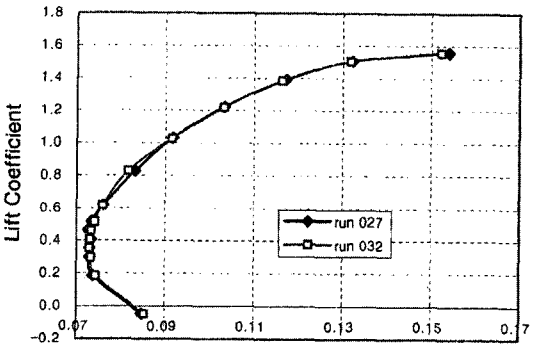

Fig. 5 Drag-polar repeatability

severe shaking at the high-angle-of-attack condition. By considering the wing geometry distortion due to air-load and vibration, the measured repeatability is reliable.

The repeatability of the pitching moment vs. lift coefficient characteristics is shown in Fig. 4. Results display a good agreement throughout −6 to 7 degrees angle-of-attack. To estimate measurement repeatability closely, data comparisons were done using the 3rd order of curve fitting. The average difference for the selected region is 0.0027, and it in turns represents 0.09 N-m. Figure 5 shows the drag-polar for two tests. The state-of-art 3rd order curve fitting from lift coefficient 0.2 to 1.4 presents less than 6 count differences for the specified lift coefficients, and drag coefficient difference corresponds to 0.1 N.

From the result of the repeatability test, one can say that the acquired data guarantees a full level of confidence, and the tunnel operating condi-

tions such as dynamic pressure and model installation are also reliable.

3.2 Model components build-up

Aerodynamic coefficient variations with model components build-up are discussed in hereby. The test started from the simple configuration, that is wing and body. The selected configurations to explore model component build-up effects are the followings; wing+body (WB), WB+tails (WBVH), WBVH with landing gear (WBVH+LG), and WBVH+test boom (WBVH+TB).

Lift coefficient variations with model component build-up is shown in Fig. 6. The lift coefficient vs. angle-of-attack of the three configurations, WBVH, WBVH+L/G and WBVH+TB, has identical slope in linear regions. Lift slope of the WBVH using the 1st order curve fitting from -8 to 6 degrees is 0.1012/deg, and installing test boom and landing gear show 0.1011/deg and 0.1016/deg respectively. Otherwise, in WB configuration the lift slope is 0. 0962/deg.

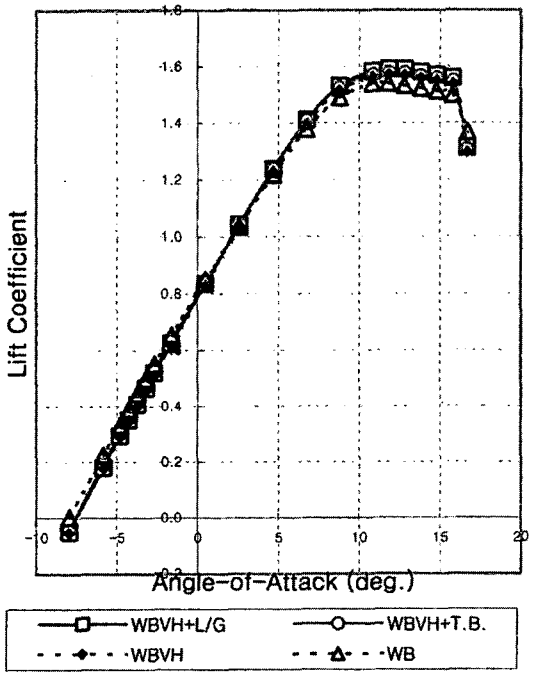

Fig. 6 Lift variation with components build-up

The pitching moment characteristics with model components build-up are shown in Fig. 7. In tail-off condition, the pitching moment change with lift coefficient is positive, pitch-up motion, and its slope is 0.0409. With installing tails, the slope is reversed in negative direction, i.e. stable, and has the value of -0.1796 from -7 to -2 degrees ranges. The effects of the test boom and landing gear do not strong enough to change the pitching moment slope with lift coefficient for the

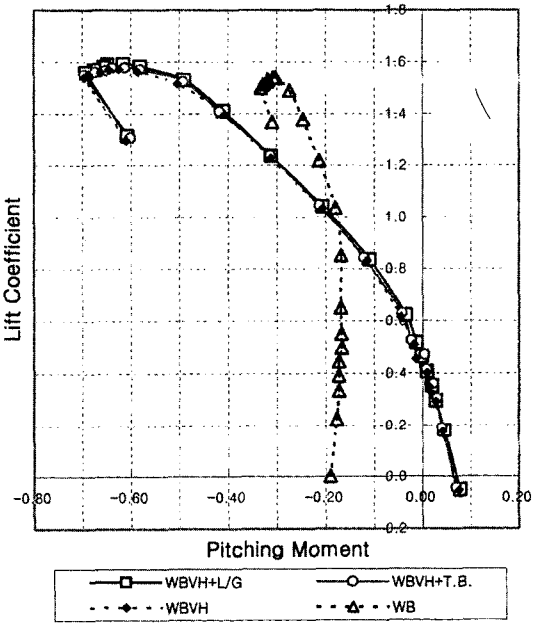

Fig. 7 Pitching moment with components build-up

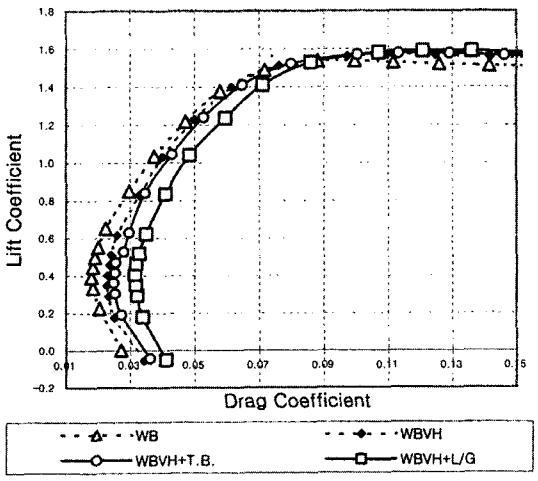

Fig. 8 Drag build-up with model components

Table 4 Drag build-up

WB	C_D=−0.0157C_L^3+0.0729C_L^2 −0.0487C_L+0.0273
WBVH	C_D=−0.013C_L^3+0.065C_L^2 −0.0443C_L+0.0313
WBVH+TB	C_D=−0.0119C_L^3+0.0627C_L^2 −0.0432C_L+0.0337
WBVH+LG	C_D=−0.0078C_L^3+0.054C_L^2 −0.038C_L+0.039

whole measurement regions.

Drag-polar characteristics of UAV with model components build-up are shown in Fig. 8. Drag enhancements with model components addition are estimated in the specific lift coefficient in where drag coefficient is minimal, and the mathematic expression for the drag-polar is the 3rd order polynomials. Compared with the WB configuration, the drag increases due to tails, tails with test boom, and tails with landing gear are 47, 72 and 135 counts respectively. The 3rd order of drag-polar for given configuration is shown in Table 4.

3.3 Control surfaces and high-lift device effects on the aerodynamic coefficients

The variation of the aerodynamic coefficients with control surface deflections is shown in Figs. 9 through 12. Figure 9 shows the behaviors of the lift coefficient according to the elevator and flap deflections and illustrates the effectiveness of elevator. Without elevator deflection, Basic (WBVH) in Fig. 9, the lift curve is positioned between −10 and 10 degrees of elevator deflection. Slopes of five elevator deflection conditions have an identical value in the linear regions of angle-of-attack, and the slope is 0.101/deg. The maximum difference in slope with elevator deflection is in order of 0.001/deg. The high-lift device, flap, increases the magnitude of lift force, the slope of lift coefficient up to 4 degrees angle-of-attack is however the same as elevator deflections.

The elevator and flap are only device to control the static longitudinal stability of an UAV, the effectiveness of those components must be examined. The pitching moment change with lift

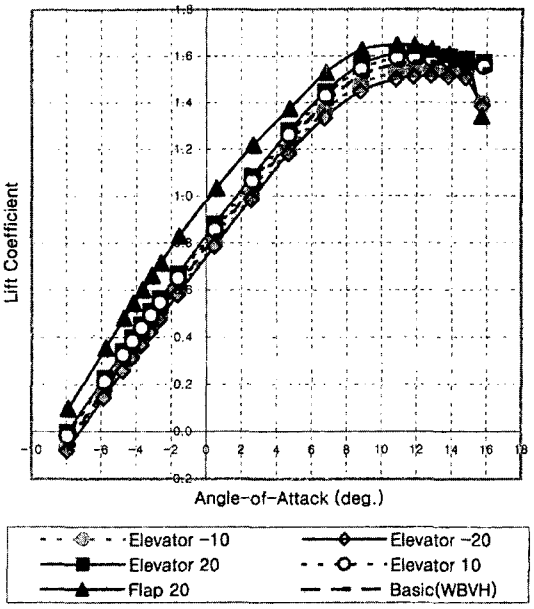

Fig. 9 Control surfaces effects on lift coefficient

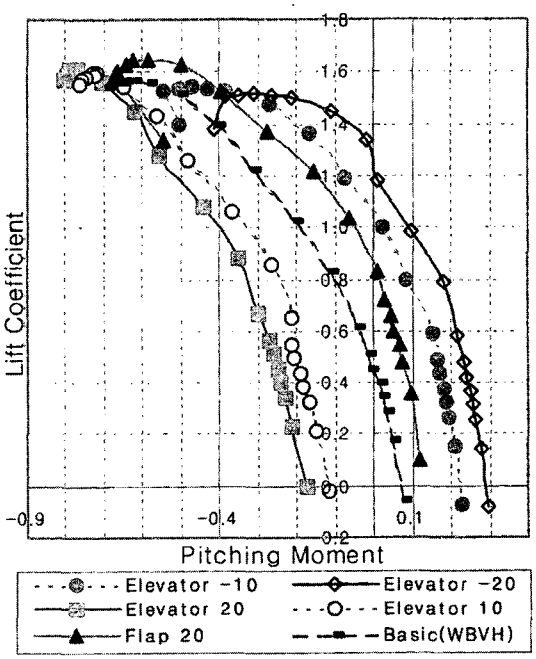

Fig. 10 Control surface effects on pitching moment

coefficient for elevator and flap deflections, shown in Fig. 10, has negative sign. The slope patterns of elevator deflections seem to be depending on its deflection direction. Slope of the positive elevator deflections has −0.17, but the

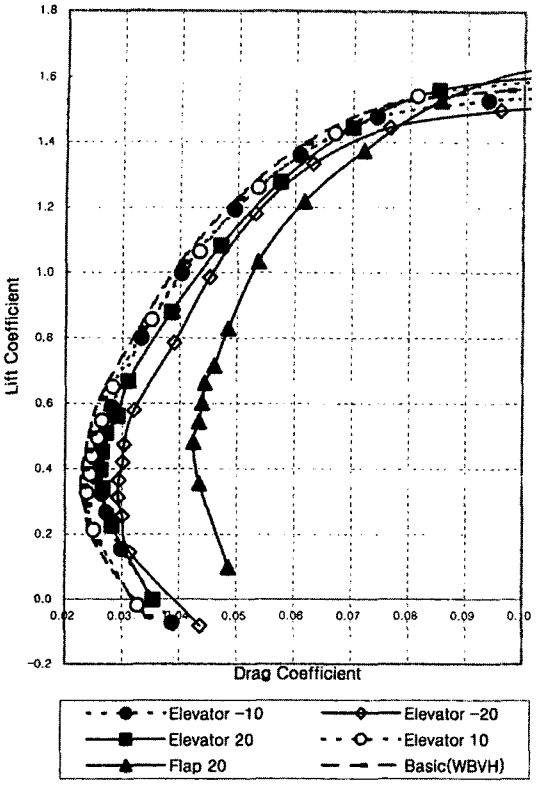

Fig. 11 Control surfaces effects on drag-polar

negative deflections have −0.13. The magnitude differences between positive and negative elevator deflections show nearly constant up to 4 degrees angle-of-attack.

Drag-polar characteristics of an UAV with elevator and flap deflections are shown in Fig. 11. Since the flow pattern around negatively deflected elevators generates more severe flow disturbance compared with positively deflected one, the negatively deflected elevators have higher drag values. And one can estimate drag coefficient using mathematical formula of drag-polar summarized in Table 5.

The variations of the yawing and rolling moments with rudder and aileron deflections are shown in Fig. 12. Yawing moment with rudder deflection represents kind of good symmetric pattern, and the minor shift from the yawing moment 0 value is related with misalignment of the model. The rolling moment of the UAV with aileron deflection illustrates that the effectiveness of aileron is limited a certain angle-of-attack regions.

Table 5 Drag-polar for elevator and flap deflections

Ele. −20	C_D=−0.0227C_L^3+0.0819C_L^2 −0.051C_L+0.0383
Ele. −10	C_D=−0.0108C_L^3+0.0621C_L^2 −0.046C_L+0.0352
Ele. 0	C_D=−0.013C_L^3+0.065C_L^2 −0.0433C_L+0.0313
Ele. 10	C_D=−0.0084C_L^3+0.0556C_L^2 −0.038C_L+0.0315
Ele. 20	C_D=−0.0125C_L^3+0.0655C_L^2 −0.045C_L+0.0351
Flap 20	C_D=−0.007C_L^3+0.0212C_L^2 −0.0263C_L+0.0505

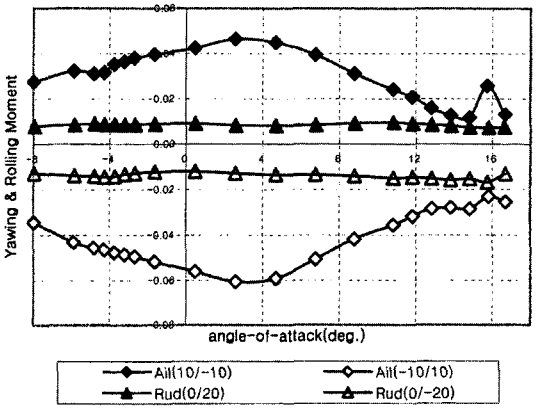

Fig. 12 Yawing and rolling moments characteristics

The aileron produces the desired rolling moment up to 3 deg.; the flourishing separation on the aileron after this gradually reduces the rolling moment. The sudden jump of rolling moment at Ail(10/−10) is caused by severe model shaking due to early stall.

4. Summary of Results

A low speed wind tunnel test was conducted to estimate the aerodynamic characteristics of the full-scale UAV having 3.2 m length of span. The drag-polar, lift and pitching moment characteristics by adding model components are illustrated. The static longitudinal stability changing elevator and flap deflection is presented. Yawing and rolling moments characteristics changing aileron and rudder deflection angles are illustrated.

In the angle-of-attack and lift coefficient relationship, lift slopes of WB and WBVH including test boom and landing gear are 0.096/deg. and 0.101/deg., respectively. The lift slope with elevator and flap deflections in the linear regions, from −6 to 5 degrees, maintains the same magnitude of WBVH configuration. The stall of the high-lift device such as flap is in general earlier than the clean configuration. However, the stall angle of the elevator and flap deflection is around 12 degrees irrespective of model configurations.

The pitching moment and lift coefficient have negative slope, stable, throughout model configurations except WB case. The general pattern of pitching moment can be divided into three regions; lift coefficient less than 0.6, between 0.6 and 1.4 and maximum lift region. The pitching moment change with lift coefficient for the positive and negative elevator deflections is −0.53 and −0.43 respectively in lift coefficient 0.6 and 1.4 regions. Drag characteristics with model components build-up, elevator and flap deflections cases are all summarized in mathematical formula. The presented 3rd order of curve fitting results can only use for lift coefficient up to 1.4.

The presented results may be useful to understand general aerodynamic characteristics and drag-polar for the given configurations.

Acknowledgment

The authors gratefully acknowledge the support of the Ministry of Science and Technology through National Research Laboratory Program.

References

Arnette, S. A., Porter, C. B., Meredith, W. S., Hoffman, J. M. and Sung, B. Z., 2000, "Aerodynamic Commissioning Results for the Korea Aerospace Research Institute Low Speed Wind Tunnel," AIAA-2000-0291, 38TH Aerospace Sciences Meeting & Exhibit, Reno, NV.

Bass, S. M., Thompson, T. L., Rutherford, J. W., 1993, "Canard Rotor/Wing : A revolutionary High-Speed Rotorcraft concept," AIAA-93-1175, Aerospace Design Conference, Irvine, CA.

Chung, J, Cho, T., Sung, B. and Lee, J, "Wind Tunnel Test of a Canard Airplane," KSME international Journal, Vol. 16, No. 1, pp. 125~131.

Helwani, M., Shockey, G. A., Smith, R. L., Thompson, T. L., 2001, "Wind Tunnel Test Results for a Canard Rotor/Wing Aircraft Configuration," 57th American Helicopter Society Meeting May 9-11.